JOURNAL OF BONE AND MINERAL RESEARCH
Volume 5, Number 3, 1990
Mary Ann Liebert, Inc., Publishers

An Automatic Method for Bone Histomorphometry: Assessment with Reference to Usual Static and Dynamic Parameters

ROBERT JUVIN,[1] EMMANUEL CAMUS,[2] YVES USSON,[2] and XAVIER PHELIP[1]

ABSTRACT

To perform a fast and reproducible analysis in bone histomorphometry, we developed an automatic method for calculating static and dynamic parameters.

A color automatic image analyzer (SAMBA 200) was used to obtain the usual parameters of bone histomorphometry: bone volume (Cn-BV%TV), osteoid volume (Cn-OV%BV), and osteoid surface (Cn-OS%BS). A specialized algorithm was designed for calculation of the mineral apposition rate (MAR). Eroded surface (Cn-ES%BS) was read in a semiautomatic mode using a cursor.

To validate this program, we input 30 samples from patients with bone disease (20 osteoporosis, 6 renal osteodystrophy, 2 osteomalacia, and 2 hyperparathyroidism) using manual and automatic modes.

The results obtained showed a highly significant correlation with the usual manual method for all parameters: OS/BS, $r = 0.93$; OV/BV, $r = 0.98$; MAR, $r = 0.90$. With the automatic method, larger values were found for osteoid parameters and MAR and lower values for BV/TV. There were no statistical differences for OV/BV and MAR when compared to the reference manual method.

This study establishes that automatic measurements of osteoid parameters and MAR can be performed by a fast analyzer with as good reproducibility and accuracy as the manual method.

INTRODUCTION

Bone histomorphometry is used for the diagnosis and assessment of osteomalacia, osteoporosis, and other metabolic bone diseases. Although it is an invasive procedure, it is the only method available for qualitative evaluation of bone remodeling. Currently, the analysis of bone samples is made by a manual method using an integrating eyepiece mounted on a microscope to measure areas and perimeters. The reproducibility of this method had been reported in several papers,[1-4] which noted significant differences for all parameters between intra- or interobserver measurements. With the development of new techniques,[5,6] a semiautomatic method was proposed that uses a cursor for marking boundaries of trabecular or osteoid surfaces.[7] Reproducibility of osteoid volume and eroded surface was unsatisfactory,[7,8] perhaps due to ill-defined boundaries or a too large cursor.

This problem can be solved by automatic image analysis: trabecular bone volume (BV/TV) can be measured with a black and white system,[9,10] and the correlation with manual or semiautomatic methods is very high. No studies have been reported on automatic measurements of osteoid parameters or mineral apposition rate (MAR). Measurement of resorption surfaces appears to be too difficult because of the lack of accurate criteria.

The purpose of this study was (1) to validate a dedicated program for automatic analysis of osteoid parameters using a color image analyzer (SAMBA-TITN), and (2) to define a new program to measure mineral apposition rate using a fluorescent marker.

[1]Clinique Rhumatologique et Hydrologique Centre Hospitalier Régional et Universitaire de Grenoble, Grenoble, France.
[2]Laboratoire TIM 3, Unité Associée CNRS no. 397, Université Joseph Fourier, Grenoble, France.

MATERIAL AND METHODS

Patients

A total of 30 samples from patients hospitalized in the department of rheumatology were studied. There were 19 women and 11 men with a mean age of 56 years (16–84 years). Diagnosis was osteoporosis for 20 patients, renal osteodystrophy for 6, osteomalacia for 2, and hyperparathyroidism for 2. Preliminary tetracycline labeling was used for 28 of the 30 patients according to the classic sequence 4-10-4 days.[11]

Transiliac bone biopsies

Iliac crest biopsies were made with a trephine of 8 mm diameter, 2 cm behind the anterior and superior iliac spine and 2 cm above the iliac crest.

Each bone core was treated in 70% ethanol without decalcification and then embedded in methylmethacrylate. Four 8 μm cross sections and three 20 μm cross sections were cut using a Jung microtome. The 8 μm sections were stained with Goldner's trichrome, coloring osteoid tissue red and calcified tissue green. The 20 μm sections reserved for fluorescence analysis were not stained.

Parameters

The following parameters were studied and expressed with surface and volume for three-dimensional values and their corresponding two-dimensional measurements with perimeter and area[12]:

Bone volume (Cn-BV%TV), expressed as a percentage of total cancellous bone volume occupied by trabeculae. In two-dimensional analysis the corresponding measurement is B.Ar/T.Ar.

Osteoid surface (Cn-OS%BS), the percentage of total cancellous bone surface covered by osteoid. In two-dimensional analysis, the corresponding measurement is O.Pm/B.Pm.

Osteoid volume (Cn-OV%BV), the percentage of total cancellous bone volume occupied by osteoid. In two-dimensional analysis, the corresponding measurement is O.Ar/B.Ar.

Eroded surfaces (Cn-ES%BS), the percentage of total cancellous bone surface showing resorption cavities with or without osteoclasts. In two-dimensional analysis, the corresponding measurement is E.Pm/B.Pm.

Mineral apposition rate expressed in micrometer per day (μm/day), which is the rate of progression of the calcification front labeled twice by tetracycline.

Manual measurements

Measurements of static parameters were made using a 100× objective. Different grid densities were used with the integrating eyepiece: a 25-point grid for BV/TV, a 100-point grid for OV/BV, and a five-line grid for OS/BS and ES/BS. Calcification fronts were revealed by fluorescence, and MAR was measured using a micrometer and a 250× objective.

Automatic measurements

The automatic analyzer, SAMBA 200 (Alcatel-TITN, Le Trident, Grenoble, France), integrates a microscope with an electro-optical image scanner including a photomultiplier, an image analysis and pattern recognition processor, a hardware processor for color analysis, and operating software including a resident statistical package.[13]

Each field, corresponding to an area of 0.78 mm^2, is displayed on a color video as an assembly of 12 subimages of 64 × 64 pixels. The size of 1 pixel is 15.9 μm^2.

Application program for B.Ar/T.Ar, O.Pm/B.Pm, and O.Ar/B.Ar measurement

Color Image Processing (Fig. 1): Three images of the same field were digitized through the red, green, and blue

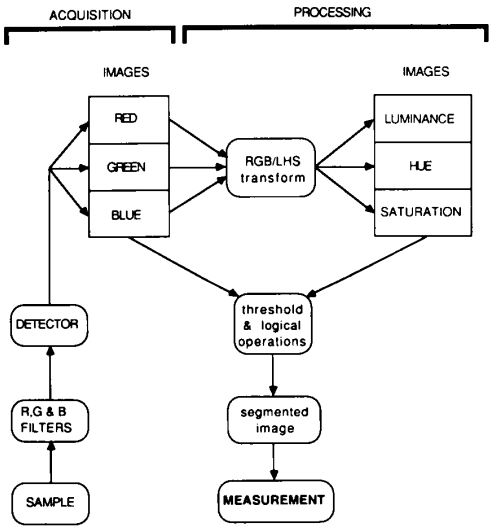

FIG. 1. Automatic measurement using SAMBA 200-TITN. Two successive procedures are applied. (1) Acquisition: images of the sample analyzed by a scanning module composed of two orthogonal vibrating mirrors. The detector is a photomultiplier that digitalizes optical densities through red, green, and blue filters, respectively. The digital images R, G, and B are stored in the common memory and are available for image processing. (2) Processing: the triplet R, G, and B is transformed by dedicated hardware into a triplet carrying information in luminance L, hue H, and saturation S. The user chooses the wavelength range to isolate each tissue color. Segmentation masks are generated by histogram thresholding of the RGB and LHS images. Shape filtering of these masks is then performed by means of morphologic transformations, such as dilatation and erosion. Surface area and length parameters are stored, and data analysis is performed using mean, standard error, and the confidence interval.

(R, G, and B) filters. A dedicated hardware processor transforms R, G, and B images into luminance (L, related to the quantity of light emitted by a colored object), hue (H, colors of rainbow range), and saturation (S, purity factor of the color) images.[14] This color model offers the advantage of being compatible with human visual experience and R, G, and B. All these transformed images are stored for further processing.

Image Segmentation (Fig. 2): Image segmentation consists in locating areas of the same image where pixels share common color properties. The analysis involves a thresholding based on the color optical density histogram. Using the latter, a single wavelength range is chosen and during segmentation only pixels belonging to these density values are retained. After tests with the six color histograms (R, G, B, L, H, and S), we finally selected the following operations:

The whole trabecular bone was segmented with the red image and a preliminary level thresholding was performed on the red optical density histogram.

The calcified bone was segmented using the hue image. A wavelength bandwidth was selected on the hue histogram.

B.Ar was obtained from the binary image after segmentation of the red image and the calculation of the corresponding area. T.Ar corresponds to the whole tissue area analyzed and is directly given by the software (Fig. 2).

Osteoid tissue was obtained by means of a logical subtraction between the binary image after hue segmentation and B.Ar.

Irregularities of the segmentation mask due to stain defects were smoothed by means of morphologic transformations using erosion and dilatation.[13]

By means of erosion, an object pixel is turned into a

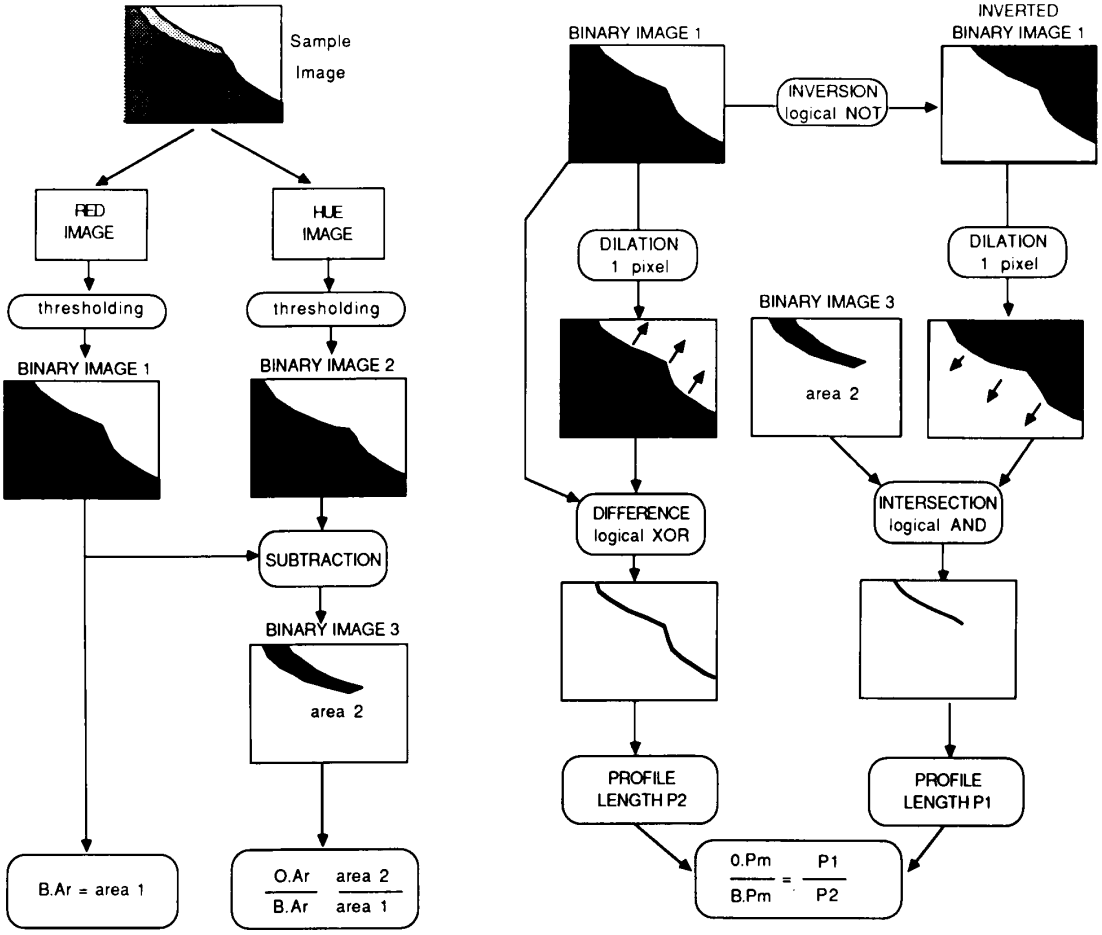

FIG. 2. Automatic program for reading BV/TV, OV/BV, and OS/BS. First, two-dimensional measurements are performed with corresponding area and perimeter: B.Ar/T.Ar, O.Ar/B.Ar, and O.Pm/B.Pm (T.Ar is directly given by the software). Thresholding permits one to select wavelength ranges corresponding to the boundaries of trabecular (red image) and calcified tissue (hue image). Series of logical and morphologic transforms are applied to the segmentation masks.

background pixel if it is surrounded by at least three background pixels, so that object pixels that originate at the boundary are deleted. By means of dilatation, a background pixel surrounded by at least three object pixels is labeled an object pixel, so that small concavities of the boundary, as well as small voids in the object, are closed. Erosion has a shaving effect; dilatation has a filling effect. These procedures are used complementarily to compensate for both the discrete transformation effect on image regularity and local color homogeneity.

O.Ar is the result of B.Ar image minus the calcified bone image, and O.Pm/B.Pm is the ratio of the perimeter of osteoid tissue (P1) to the perimeter of total trabecular bone (P2).

A magnification factor of 100 was used.

Parametrization: Two parameters were calculated on the binary images: area and perimeter, expressed as number of pixels.

Application program for mineral apposition rate

The mineral apposition rate was studied using the SAMBA 2002 system, which provides direct input for a video camera. The size of the elementary field is 512 × 512, permitting greater accuracy and faster analysis. All fluorescent sites were studied at ×540 magnification. We applied the same method as described by Frost[11]: four measures were made on the same fluorescent label at different locations. We analyzed only labels with sufficient brightness, that is, when lines were well separated and without discontinuities.

Measurement of the mean distance between two fluorescent lines is made from the middle of the inner line to the middle of the outer line. After segmentation, two binary images are obtained (Fig. 3): the first represents the surface between the outer side of the two lines, the second, the surface between the inner side of the two lines. On each image, an algorithm searches for the main orientation (D_i) of the surface and then calculates the average width along the orthogonal direction. The mean of the two results (W_1 and W_2) is the mean distance between two fluorescent lines. Therefore, the calcification rate can be derived from the measurements with respect to the size of one pixel and the sequence of tetracycline labeling.

Correction of obliquity was not included in our program, but a sampling strategy may be used to reduce this defect: a correction factor of 0.79 is proposed to multiply by the mean value between the two fluorescent labels, to control differences between the plane of the bone section and the plane of the bone-forming surface.[15]

Application program for eroded perimeter (E.Pm/B.Pm)

E.Pm/B.Pm was measured in the interactive mode using a digitizing pad for outlining the contours of selected surfaces that are directly superimposed on the image to be analyzed.

We used ×100 magnification.

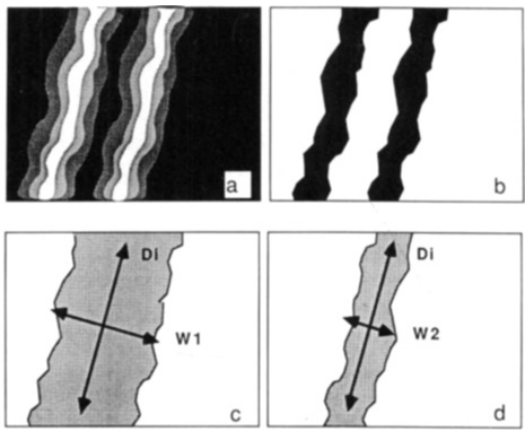

FIG. 3. Measurement of mineral apposition rate (MAR) using fluorescent light at ×500. After acquisition and gray-level thresholding, two bands corresponding to the mineralization lines are displayed in A and B. Two segmentation masks are generated: one surface area delimited by the outer lines of the two bands (C) and one surface area delimited by the inner line of the two bands (D). The width between outer lines (W_1) and the width between inner lines (W_2) are measured orthogonally to the main direction D_i. MAR is obtained by $(W_1 + W_2)/2$.

Protocol

All samples were manually input by the same observer.

To establish the interobserver difference, five osteoporotic biopsy samples were chosen according to following criteria:

It is the most frequently encountered pathology in osseous diseases.

There is only a small amount of osteoid tissue, and identification of the boundaries of this tissue is difficult. This gives a good indication of the interobserver error; the same argument holds for eroded surfaces, thus underscoring the discrepancy of the boundary assessment by different observers.

Finally, measurements were made on the 30 samples with our automatic program and the semiautomatic method for ES/BS. For each biopsy, four samples 8 μm thick were stained with Goldner's trichrome. The same tissue areas per individual were analyzed with the manual and automatic methods. The sections were systematically and completely scanned in a serpentine manner,[16] starting from the right upper trabecular space of each section to the opposite left lower trabecular space.

Only 10 biopsies were read in automatic mode using fluorescent light.

TABLE 1. VALUES OF HISTOMORPHOMETRIC PARAMETERS FOR THE MANUAL (M) AND AUTOMATIC (A) READINGS FOR 30 SAMPLES FROM PATIENTS WITH BONE DISEASES

Patients		*Cn-BV%TV*	*Cn-OV%BV*	*Cn-OS%BS*	*Cn-ES%BS*	*MAR (μm/day)*
Osteoporosis						
1	A	10.28	8.71	52.90	11.20	
	M	14.88	10.00	55.83	9.74	
2	A	5.89	2.34	12.32	0.98	
	M	6.05	2.12	18.25	1.44	
3	A	14.17	5.64	45.85	2.67	
	M	14.25	6.68	30.91	3.24	
4	A	13.13	3.17	25.47	1.56	
	M	16.36	4.06	16.88	1.80	
5	A	8.21	6.85	31.38	15.31	1.26
	M	8.98	6.99	31.32	11.40	0.98
6	A	11.12	4.65	21.00	10.32	0.86
	M	11.06	4.82	21.97	8.88	1.04
7	A	10.85	3.40	24.37	4.32	
	M	11.72	4.05	23.52	4.83	
8	A	17.02	1.17	13.53	3.02	
	M	19.53	1.56	9.78	3.60	
9	A	18.78	7.96	31.44	3.96	
	M	18.80	6.92	28.32	4.32	
10	A	10.58	4.19	30.44	5.88	
	M	12.18	3.48	21.00	5.64	
11	A	17.51	3.94	30.49	3.25	
	M	17.31	3.78	25.57	3.72	
12	A	7.76	1.06	15.22	2.18	
	M	10.24	0.85	8.56	2.52	
13	A	7.49	4.30	17.89	1.71	
	M	10.61	5.38	16.06	2.28	
14	A	12.23	4.38	42.46	7.68	
	M	15.33	4.95	29.30	5.88	
15	A	18.21	1.57	16.09	3.36	
	M	18.85	2.25	14.54	5.40	
16	A	16.95	1.86	18.48	2.89	1.01
	M	14.03	2.23	11.35	2.52	1.03
17	A	19.90	1.65	13.28	0.60	
	M	18.57	2.56	15.00	0.72	
18	A	11.77	1.32	10.36	3.84	0.64
	M	12.88	1.59	9.20	3.61	0.59
19	A	10.66	4.46	24.96	2.34	0.76
	M	10.30	4.91	23.28	2.77	0.60
20	A	12.20	4.28	29.41	0.97	
	M	12.73	5.20	22.44	1.45	
Renal osteodystrophy						
21	A	21.09	7.53	67.72	31.44	
	M	25.42	7.26	64.80	23.52	
22	A	26.58	17.37	73.90	23.16	
	M	30.33	12.30	52.21	18.84	
23	A	18.56	7.37	59.32	18.03	1.16
	M	19.80	7.11	48.16	15.48	1.10
24	A	24.17	4.85	33.06	0.84	0.92
	M	23.15	4.06	43.35	1.21	0.74
25	A	17.20	3.24	34.77	1.16	0.84
	M	14.85	4.82	23.02	1.44	0.65
26	A	26.97	3.56	29.40	2.58	
	M	26.70	4.29	19.32	2.44	
Hyperparathyroidism						
27	A	20.12	5.64	37.24	26.43	1.06
	M	21.92	6.97	44.73	24.60	0.94
28	A	50.06	6.46	64.59	47.76	1.62
	M	54.14	8.08	59.10	41.88	1.77
Osteomalacia						
29	A	14.36	56.95	86.23	8.88	
	M	11.00	52.50	98.20	9.84	
30	A	12.14	23.20	88.77	23.76	
	M	14.06	14.35	86.41	16.32	

Tissue area evaluated per biopsy was 12 fields of 0.78 mm^2 from each of four sections, accounting for a total area of 37.5 mm^2 per individual.

Data are expressed in three-dimensional measurements with volume and surface. They are derived from two-dimensional measurements multiplying by 1.2 for OS/BS, ES/BS. BV/TV and OV/BV are numerically identical to B.Ar/T.Ar and O.Ar/B.Ar.[12]

Statistical analysis

Results are expressed as the mean ± standard deviation (SD).

The difference between the two means is expressed as percentage of the manual method, which is the reference method. Variation between the two methods was measured using intrapair standard deviation: $S = \sqrt{d^2/2n}$, where d is the difference between two measurements for one biopsy and n is the number of biopsies; the intrapair coefficient of variation CV = S/M × 100, where M is the total mean of the average of two measures on the same biopsy.[17]

Analysis of variance (repeated measures one-factor ANOVA) was performed to compare the two methods.

Normality of distribution was verified before statistical tests were used.

Comparison between the two means was made using Student's t-test.

The relation between the two methods was obtained by regression analysis.

RESULTS

Measurements obtained with both techniques for all patients are shown in Table 1.

Interobserver variations

A significant correlation exists between the two observers (Tables 2 and 3). For osteoid parameters, the interobserver variation is much larger than the intermethod variation.

Intermethod variation (Table 4)

A highly significant correlation between the two methods was found for all parameters, with r values from 0.93 to 0.99 (Fig. 4). The highest correlation values were observed for BV/TV (0.97) and OV/BV (0.99).

For BV/TV, there was a significant difference (5.53 ± 13.58), with larger values for manual measurement but with a low intrapair CV (9.58%). Analysis of variance confirmed these results ($p < 0.01$).

For osteoid analysis, we found larger values for the automatic method and a high intrapair CV. Intrapair SD was high for both parameters. There was a statistically significant difference for OS/BS (17.40 ± 35.53) but not for OV/BV (2.22 ± 22.76). Analysis of variance showed the same results, with $p < 0.05$ for OS/BS.

For ES/BS, large differences were observed between the two methods when measurements with high values were considered. No such differences were obtained for low val-

TABLE 2. CORRELATION BETWEEN THE AUTOMATIC ANALYSIS AND INTEGRATING EYEPIECE FOR THE TRABECULAR AND OSTEOID PARAMETERS IN FIVE BIOPSIES FROM OSTEOPOROTIC PATIENTS[a]

	Correlation coefficient		
Parameters	*Manual 1 versus manual 2*	*Manual 1 versus automatic*	*Manual 2 versus automatic*
Cn-BV%TV	0.98[b]	0.94[b]	0.97[b]
Cn-OS%BS	0.97[b]	0.95[b]	0.93[c]
Cn-OV%BV	0.96[b]	0.97[b]	0.99[b]

[a]First observer, manual 1; second observer, manual 2.
[b]$p < 0.01$.
[c]$p < 0.05$.

TABLE 3. INTERMETHOD VARIATION OF BV/TV AND OSTEOID PARAMETERS IN FIVE BIOPSIES FROM OSTEOPOROTIC PATIENTS[a]

Parameters (n = 5)	*Manual 1*	*Manual 2*	S	*CV (%)*	r
Cn-BV%TV	10.00 ± 2.76	9.85 ± 2.55	0.33	3.33	0.98
Cn-OS%BS	23.07 ± 10.8	20.79 ± 8.11	2.65	12.00	0.97
Cn-OV%BV	4.19 ± 2.67	4.08 ± 2.22	0.50	12.10	0.96
Parameters (n = 5)	*Manual 2*	*Automatic*	S	*CV (%)*	r
Cn-BV%TV	9.85 ± 2.55	9.53 ± 2.44	0.44	4.54	0.97
Cn-OS%BS	20.79 ± 8.11	19.88 ± 8.74	1.99	9.81	0.93
Cn-OV%BV	4.08 ± 2.22	3.92 ± 2.16	0.18	4.50	0.99

[a]S, intrapair standard deviation; CV, coefficient of variation.

TABLE 4. INTERMETHOD VARIATION OF BONE HISTOMORPHOMETRIC PARAMETERS OF 30 SAMPLES FROM PATIENTS WITH BONE DISEASES[a]

Parameters (n = *30*)	*Manual*	*Automatic*	*Difference*	*Intrapair standard deviation (S)*	*Intrapair CV (%)*	*Analysis of variance*		
						Sum of squares		F *test, manual versus automatic*
						Inter-method	*Residual*	
Bone volume Cn-BV%TV	17.28 ± 8.89	16.36 ± 8.38	5.53 ± 13.58[b]	1.60	9.58	15.07	62.714	6.969[b]
Osteoid surface Cn-OB%BS	32.77 ± 23.07	36.07 ± 21.99	−17.40 ± 35.53[c]	6.24	18.12	163.614	1025.90	4.625[c]
Osteoid volume Cn-OV%BV	6.87 ± 9.15	7.10 ± 10.48	2.22 ± 22.76	1.53	21.19	0.805	70.156	0.333
Mineral apposition rate, μm/day (MAR; n = 10)	0.94 ± 0.34	1.01 ± 0.28	−10.75 ± 16.48	0.06	6.18	0.24	0.1	2.135
Eroded surface	7.96 ± 9.22	9.06 ± 11.06	27.46 ± 26.37[c]	1.87	21.94	15.79	90.171	5.08[c]

[a] *S*, intrapair standard deviation; CV, coefficient of variation.
[b] $p < 0.01$.
[c] $p < 0.05$.

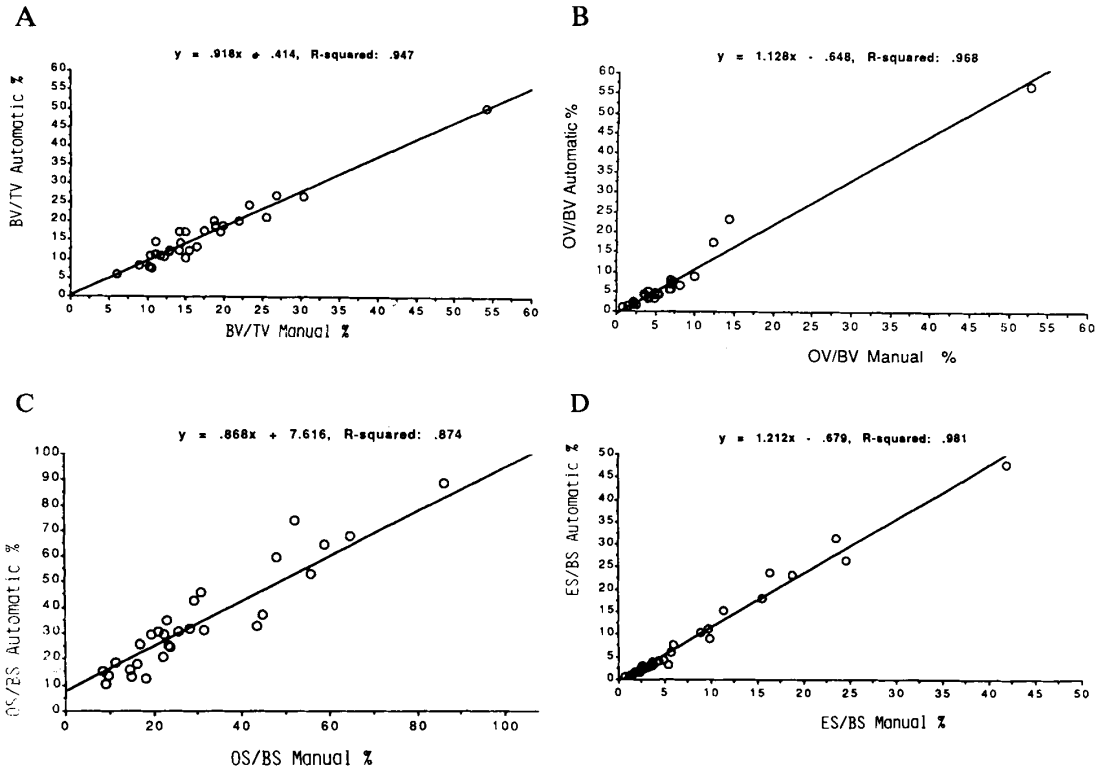

FIG. 4. Relationships between manual and automatic analysis of the 30 samples: (A) Cn-BV%TV (r = 0.97). (B) Cn-OV%BV (r = 0.98). (C) Cn-OS%BS (r = 0.93). (D) Cn-ES%BS (r = 0.99).

ues. However, the correlation between the methods remained high.

MAR values obtained with the automatic method were larger than with the manual method. However, the differences were not statistically significant. The intrapair CV of MAR was the lowest observed among all parameters (6.18%).

DISCUSSION

In this study we assessed the automatic reading of osteoid parameters based on color data and mineral apposition rate using an image analyzer. A close correlation with manual measurements was found.

This is the first report of automatic reading for bone histomorphometric parameters using color information. Another comparison between the two methods has been reported by Chavassieux et al.,[7] but their work was concerned only with BV/TV; the other parameters were measured with a semiautomatic method. In that paper BV/TV measurements were obtained using a noncolor system (Quantimet) at ×40 magnification, and samples were stained with solochrome cyanine. These authors found a difference between the two methods: the intrapair CV was 6.2%, and correlation was 0.93. We found a greater difference but a similar intrapair CV and a better r value.

The discrepancy between these results can be explained by the better resolution of our method due to the use of a higher magnification and color data. The latter is a very good tool for segmenting the boundaries of calcified bone from osteoid bone. We observed that variations seemed to be larger when larger volumes of osteoid tissue were considered.

The largest difference between manual and automatic methods was observed for the OS/BS parameter. However, we retained only osteoid surfaces larger than one osteoid lamella at this magnification. Furthermore, dilatation and erosion were used to remove some stain artifacts. Perhaps the initial thresholding using the red filter overestimated osteoid tissue. The density threshold used to define calcified bone limits may have balanced the small values found for BV/TV. The trabecular perimeter P2 (Fig. 2), like BV/TV, had smaller values, emphasizing the OS/BS difference.

OV/BV results showed no significant difference between the two methods, but Fig. 4 shows that high values of OV/BV are scattered with larger values for automatic method. The high correlation for low values of this parameter should be noted.

The difference between the two methods for osteoid parameters can be minimized, since method SD are high (Table 4). With interactive measurements,[7] there were smaller values for osteoid parameters, but the measurement variation was the same: intrapair CV was 18.4% for OS/BS and 25.2% for OV/BV. The difficulty of manual reading of osteoid parameters should be kept in mind: 100% variation was recorded between four observers for OS/BS[3]; in another study CV was 51.8% for OS/BS and 68.7% for OV/BV[2]; a result of 23% interobserver variance for OS/BS was also found.[1]

In this study, an original automatic reading of mineral apposition rate was obtained with a significant correlation with the manual method, although automatic values were higher. Sontag[18] proposed an experimental method for the rat that required two consecutive inputs of the samples: the first to measure the intensity of fluorescence and the second to measure interline distances after staining with alizarin red. Our automatic method, which uses a single analysis, avoids the two-procedure protocol. Measurements of the mean distance between two tetracycline labels were also performed using a semiautomatic method,[8] with a good reproducibility.

Overestimation by the automatic program can be explained by the difficulty of finding a satisfactory threshold. The fluorescent lines have fuzzy margins, and their widths tend to be significantly widened by a small variation in the threshold. Contiguous labeling cannot be measured by this method.

Fully automatic readings could not be achieved since it was necessary to locate fluorescent labels with a 100× lens before automatic analysis at ×500. Our program could be improved to automatically handle the positioning of the fluorescent labels.

For ES/BS, our semiautomatic digitization is in accord with the literature.[7,8] Assessment of resorption boundaries is difficult and explains the differences between the methods.

In our study, a manual method was used as a reference method. However, this method is not absolute since it shows poor reproducibility. We think that our data show that the automatic method, with its resolution and precision, is more accurate than the manual method.

The automatic method gives the clinician a fast and efficient tool for the reading of bone biopsies and, above all, better reproducibility, permitting standardization of methods and facilitating comparisons of results between research centers. Integration of other stains, such as acid phosphatase or toluidine blue, will allow the study of cytologic parameters for osteoblasts and osteoclasts and other histologic parameters, such as eroded surfaces and mean wall thickness (using polarized light).

ACKNOWLEDGMENTS

We are indebted to Prof. G. Brugal for advice. We would like to thank Dr. D. Blanc, Ms. B. Batteux for preparing samples, Mrs. R. Giroud for preparation of the manuscript, and Mrs. V. Von Hagen for kind review of the manuscript.

REFERENCES

1. Birkenhager-Frenkel DM, Schmitz PIM, Breuls PN 1976 Biological variation as compared to inter observer variation and instrinsic error of measurement, for some parameters, within single bone biopsies. In: Meunier PJ (ed) Bone Histomorphometry, Second International Workshop, pp. 63–67.
2. Compston JE, Vedi S, Stellon AJ 1986 Interobserver and intra-observer variation in bone histomorphometry. Calcif Tissue Int **38**:67–70.
3. Delling G, Luehmann M, Baron R, Mathews CHE, Olah A 1980 Investigation of intra and inter reader reproducibility. In: Jee WSS, Parfitt AM (ed) Bone Histomorphometry, Third international Workshop, pp. 419–427.
4. De Vernejoul MC, Kuntz D, Miravet L, Goutallier D, Rickewaert A 1981 Bone histomorphometric reproducibility in normal patients. Calcif Tissue Int **33**:369–374.
5. Morey ER, Wronski TJ 1980 Digital image processing of bone: Problems and potentials. In: Jee WSS, Parfitt AM (ed) Bone Histomorphometry, Third International Workshop, Sun Valley, pp. 463–468.
6. Smith JM, Jee WSS 1983 Automated skeletal histomorphometry. In: Recker RR (ed) Bone Histomorphometry: Techniques and Interpretation. Boca Raton, FL: CRC Press, pp. 285–294.
7. Chavassieux PM, Arlot ME, Meunier PJ 1985 Intermethod variation in bone histomorphometry: Comparison between manual and computerized methods applied to iliac bone biopsies. Bone **6**:221–229.
8. Malluche HH, Sherman D, Meyer W, Massry SG 1982 A new semiautomatic method for quantitative static and dynamic bone histology. Calcif Tissue Int **34**:439–448.
9. Beisbeder M, Chappard D, Alexandre C, Vico L, Palle S, Riffat G 1988 Improved algorithms for automatic bone histomorphometry on a numerized image analysis system. J Microsc **150**:151–160.
10. Meunier PJ 1973 Use of an image analysing computer for bone morphometry. In: Frame B, Parfitt AM, Duncan H (ed) Clinical Aspects of Metabolic Bone Diseases. Amsterdam: Excerpta Medica, pp. 148–151.
11. Frost HM 1969 Tetracycline base histological analysis of bone remodeling. Calcif Tissue Res **3**:211–237.
12. Parfitt AM, Drezner MC, Glorieux FH, Kanis JA, Malluche H, Meunier PJ, Ott SM, Recker RR 1987 Bone histomorphometry: Standardization of nomenclature, symbols, and units. J Bone Min Res **2**:595–700.
13. Brugal G 1986 Image analysis of microscopic preparation. Methods Achiev Exp Pathol **11**:1–33.
14. Garbay C, Brugal G, Choquet C 1981 Application of colored image analysis to bone marrow cell recognition. Analyt Quant Cytol **3**:272–280.

15. Frost HM 1983 Bone histomorphometry: Analysis of trabecular bone dynamics. In: Recker RR (ed) Histomorphometry: Techniques and Interpretation. Boca Raton, FL: CRC Press, pp. 109–131.
16. Torch S, Stoebner P, Usson Y, Drouet D'Aubigny G, Saxod R 1989 There is no simple adequate sampling scheme for estimating the myelinated fibre size distribution in human peripheral nerve: A statistical ultrastructural study. J Neurosci Methods 27:149–164.
17. Sokal RR, Rohlf FJ 1981 Biometry, The Principles and Practice of Statistics in Biological Research, Freeman Edt.
18. Sontag W 1980 An automatic microspectrophotometric scanning method for the measurement of bone remodeling rate in vivo. Calcif Tissue Int 32:63–68.

Address reprint requests to:
Dr. R. Juvin
Clinique Rhumatologique
Centre Hospitalier Régional et Universitaire de Grenoble
BP 217X, 38043 Grenoble Cedex, France

Received for publication March 20, 1989; in revised form August 28, 1989; accepted August 29, 1989.